

Influence of the polymer concentration on the electroluminescence of ZnO nanorod/polymer hybrid light emitting diodes

Siama Zaman, Ahmed Zainelabdin, Gul Amin, Omer Nour and Magnus Willander

Linköping University Post Print

N.B.: When citing this work, cite the original article.

Original Publication:

Siama Zaman, Ahmed Zainelabdin, Gul Amin, Omer Nour and Magnus Willander, Influence of the polymer concentration on the electroluminescence of ZnO nanorod/polymer hybrid light emitting diodes, 2012, Journal of Applied Physics, (112), 6, 064324.

<http://dx.doi.org/10.1063/1.4754542>

Copyright: American Institute of Physics (AIP)

<http://www.aip.org/>

Postprint available at: Linköping University Electronic Press

<http://urn.kb.se/resolve?urn=urn:nbn:se:liu:diva-81426>

Influence of the polymer concentration on the electroluminescence of ZnO nanorod/polymer hybrid light emitting diodes

Saima Zaman,^{a)} Ahmed Zainelabdin, Gul Amin, Omer Nur, and Magnus Willander
Department of Science and Technology, Linköping University, 601 74 Norrköping, Sweden

(Received 11 April 2012; accepted 24 August 2012; published online 27 September 2012)

The effects of the polymer concentration on the performance of hybrid light emitting diodes (LEDs) based on zinc oxide nanorods (ZnO NRs) and poly(9,9-dioctylfluorene) (PFO) were investigated. Various characterization techniques were applied to study the performance of the PFO/ZnO NR hybrid LEDs fabricated with various PFO concentrations. The fabricated hybrid LEDs demonstrated stable rectifying diode behavior, and it was observed that the turn-on voltage of the LEDs is concentration dependent. The measured room temperature electroluminescence (EL) showed that the PFO concentration plays a critical role in the emission spectra of the hybrid LEDs. At lower PFO concentrations of 2-6 mg/ml, the EL spectra are dominated by blue emission. However, by increasing the concentration to more than 8 mg/ml, the blue emission was completely suppressed while the green emission was dominant. This EL behavior was explained by a double trap system of excitons that were trapped in the β -phase and/or in the fluorenone defects in the PFO side. The effects of current injection on the hybrid LEDs and on the EL emission were also investigated. Under a high injection current, a new blue peak was observed in the EL spectrum, which was correlated to the creation of a new chemical species on the PFO chain. The green emission peak was also enhanced with increasing injection current because of the fluorenone defects. These results indicate that the emission spectra of the hybrid LEDs can be tuned by using different polymer concentrations and by varying the current injected into the device. © 2012 American Institute of Physics. [<http://dx.doi.org/10.1063/1.4754542>]

I. INTRODUCTION

Zinc oxide (ZnO) is a II-VI semiconductor with a large direct band gap of 3.37 eV and a relatively large exciton binding energy of 60 meV with many interesting electro-optical properties.¹ ZnO has become a very attractive material for nanostructure applications, providing simple growth procedures on almost any underlying surface because of its self-organized growth property.² One promising technique for growth of ZnO nanostructures is the use of the chemical bath method, which is a low growth temperature method that can easily be scaled up for large area applications.³ This process yields ZnO in nanostructure form and enables the application of ZnO nanorods (NRs) on polymer substrates.⁴

Since the ZnO NR/polymer hybrid light emitting diode (LED) was first reported by Könenkamp *et al.*,⁵ many articles have described various LEDs based on ZnO NR/polymer heterojunctions.⁶⁻⁹ Different polymers were used to fabricate these devices and the most intensively studied polymers in connection with ZnO are PEDOT:PSS and polyfluorene (PFO). PFO is well known for its blue emission together with interesting electrical and electro-optical properties, making it suitable for polymer light emitting diode applications.^{10,11} PFO also has a simple chemical structure but is rich in morphological features, depending on the processing conditions used, which can affect the device performance and the emission color.¹² It should be noted that polymer LEDs suffer from several disadvantages, including the lack

of the stable n-type polymer necessary for device efficiency and long-term operational stability.¹³ In contrast, ZnO is an inorganic semiconductor with high electron mobility and superior stability for long-term operation. However, in contrast to organic polymers, ZnO intrinsically possesses an n-type tendency and efficient ZnO p-type doping with good reproducibility has thus far been difficult to attain.¹⁴ The combination of inorganic ZnO with organic polymers can pave the way toward large area lighting applications with simple fabrication strategies.

Previous reports on PFO/ZnO NR-based hybrid LEDs demonstrated their fabrication and white light electroluminescence (EL) by using a single PFO layer or by blending two polymers. However, the effects of the polymer thickness and of the variation of the injected current on the electrical and emission properties of PFO/ZnO NR-based hybrid LEDs were not investigated.^{15,16} In this paper, we report on the effects of the PFO concentration on the overall performance of a hybrid white light emitting diode fabricated using ZnO NRs grown at 50 °C on PFO/PEDOT:PSS multilayered polymers on flexible plastic substrates. Large electro-optical performance variations were found when varying the PFO concentration from 2 mg/ml up to 20 mg/ml. These changes were investigated with respect to the defect formation in the PFO side. The effect of the injected current on the electroluminescence spectra of the LEDs has also been studied.

II. EXPERIMENTAL PROCEDURES

Poly(9,9-dioctylfluorenyl-2,7-diyl) end capped with dimethylphenyl, or PFO, was purchased from American

^{a)}saiza@itn.liu.se.

Dye Source (ADS 129BE) and was used as-received. A commercial PEDOT:PSS coated flexible plastic was used to act as the hole injection electrode for the PFO layer. Zinc nitrate hexahydrate ($\text{Zn}(\text{NO}_3)_2 \cdot 6\text{H}_2\text{O}$) and hexamethylenetetramine (HMT, $\text{C}_6\text{H}_{12}\text{N}_4$) as purchased from Sigma-Aldrich were of analytical reagent grade and were used without further purification.

The fabrication of the hybrid LEDs begins with standard chemical cleaning of the PEDOT:PSS flexible plastic substrates in an ultrasonic bath. The PFO solutions were prepared by dissolution at concentrations of 2, 4, 6, 8, 10, and 20 mg/ml in toluene under ultrasonic agitation for 5 min, and they were then spin coated on the PEDOT:PSS plastic substrates at a spin speed of 2000 rpm (revolutions per minute) for 40 s, followed by soft baking for 10 min at 75 °C.

The growth procedure for the ZnO NRs was initiated by spin coating of a nucleation ZnO nanoparticle (NP) solution prepared by following the procedure described in our earlier work.⁴ The NPs were spin coated on the multilayer polymer flexible substrates. At the same time, an aqueous solution of zinc nitrate and HMT was prepared by dissolving equimolar amounts of 0.15M of each chemical in 200 ml of deionized water. Finally, the substrates were immersed horizontally into the aqueous solution and loaded into a laboratory oven set at 50 °C for several hours. The as-grown samples were then rinsed in deionized water to remove any residual salt, and were blown dry with a N_2 gun.

A photoresist (Shipley S1818) was spin coated on top of the hybrid LEDs to insulate the individual ZnO NRs from each other, at a spin speed of 3000 rpm and then baked for 2 min at 90 °C. An oxygen reactive ion etch (RIE) was applied to partially remove the photoresist coverage on the ZnO NR tips to allow top contact deposition. Finally, an aluminum (Al) thin film (30 nm) was thermally evaporated through a shadow mask with a circular shape. A simple silver (Ag) paint was used to form the hole injection contact layer.

The fabricated hybrid LEDs were subjected to various characterization techniques, including surface profiling (Veeco Dektak 3 ST) for polymer thickness measurements, and scanning electron microscopy (SEM) to investigate the morphology of the grown ZnO NRs. An Agilent 4155B semiconductor parameter analyzer was used to study the current-voltage (I-V) characteristics of the fabricated LEDs. A Perkin Elmer Lambda 900 UV-VIS-NIR spectrometer was used to analyze the PFO absorption properties, and an Andor Shamrock 303iB spectrometer supported with an Andor-Newton Du-790N CCD was used to investigate the EL characteristics of the LEDs, which were biased using a Keithley 2400 source meter.

III. RESULTS AND DISCUSSION

A schematic diagram of the PFO/ZnO flexible hybrid LEDs is shown in Fig. 1(a), illustrating the different polymer layers on the flexible plastic foil. The thickness of the PEDOT:PSS layer was found to be ~60 nm, while the thicknesses of the PFO layer ranged from ~29.1 nm for the 2 mg/ml concentration to ~300 nm for the 20 mg/ml concentration.

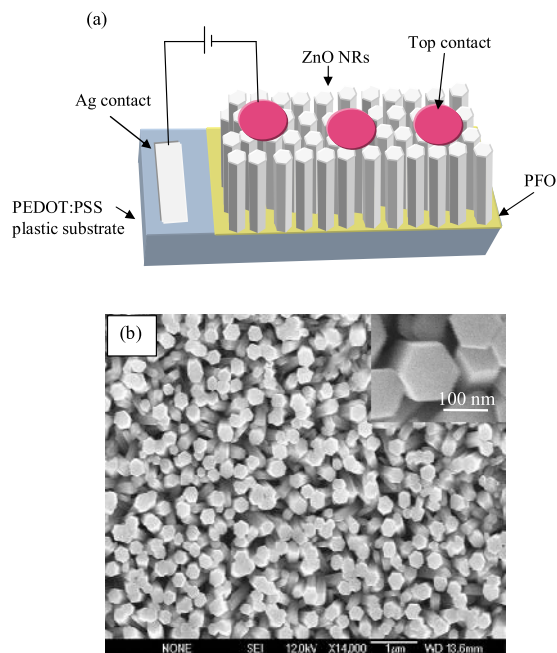


FIG. 1. (a) Schematic diagram of the hybrid light emitting diode showing the structure of the fabricated device. (b) Field emission SEM micrographs of ZnO nanorods grown on the PFO polymer layers on top of a PEDOT:PSS plastic flexible substrate.

It was noted that as the PFO concentration increased from 2 to 20 mg/ml, the coated PFO thin films became increasingly rough and large parts of the PFO were coiled. The resulting thin films therefore contained hill-and-valley shaped areas which strongly affected the subsequent growth of the ZnO NRs. In Fig. 1(b), an overview SEM micrograph of ZnO NRs grown at 50 °C on a PFO (2 mg/ml) coated plastic substrate is shown. The growth of ZnO NRs at this low temperature produces good quality NRs with high c-axis orientation, as we reported previously.⁴ The average diameter of the ZnO NRs is between 100 and 150 nm, as shown in the inset of Fig. 1(b). The axial length of these NRs is approximately 2.3 μm , demonstrating a high average aspect ratio of ~16.

The UV-VIS absorption spectra of the various PFO layers spin coated on PEDOT:PSS are shown in Fig. 2. The relative absorption intensities increase with increasing PFO concentration from 2 to 20 mg/ml. PFO has a broad absorption peak centered at ~390 nm which is attributed to the π - π^* electronic transition. This broad absorption curve is characteristic of polyfluorene polymers and is termed the glassy phase or α -phase.¹⁷ At higher concentrations, a fraction of the glassy phase (α -phase) of PFO starts to crystallize into an aggregated state termed the β -phase, as shown in Fig. 2. The occurrence of the β -phase is characterized by an absorption peak at ~436 nm.¹⁸ β -phase formation occurs as a result of the crystallization of the n-alkyl side-chains, forcing the polymer main chains into a coplanar arrangement of the fluorene building blocks. This process increases the length of the π -conjugation along the polyfluorene main-chain.¹⁹ Figure 2 shows that at the lower PFO concentrations (2 mg and 4 mg), only the α -phase (amorphous state) is present. The characteristic peak of the β -phase emerged as a shoulder at 437 nm for PFO concentrations

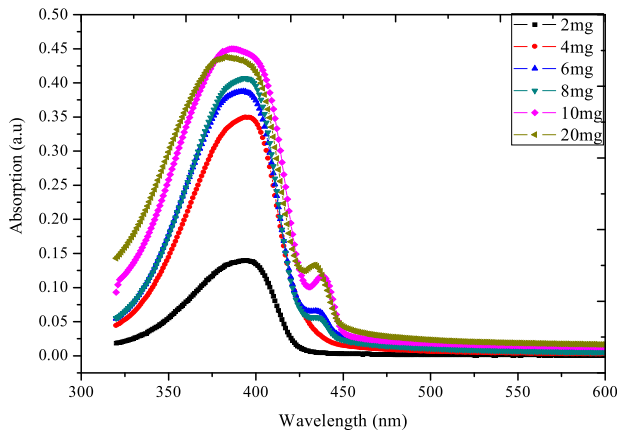


FIG. 2. UV-Visible absorption spectra of all LEDs.

higher than 6 mg/ml and then became stronger as the concentration increased up to 20 mg/ml.

The current-voltage (I-V) characteristics of the fabricated hybrid LEDs are shown in Figs. 3(a) and 3(b) for the different PFO concentrations. Figure 3(a) represents the I-V characteristics of the device with the lowest PFO concentrations. The I-V curve reveals excellent and stable rectifying diode behavior with a turn-on voltage of approximately 3.45 V and a rectification ratio of ~ 7.6 at 5 V. The ideality factor was calculated to be $\eta = 2.93$; a higher ideality factor value is frequently associated with ZnO/polymer hybrid heterojunctions.²⁰ The log scale plot of the I-V curve is shown in the inset of Fig. 3(a), which was used to deduce the η value. The processes involved in the current injection can be described as follows. Each of the LEDs has a multilayered structure of Ag/PEDOT/PFO/ZnO/Al; the electrons are injected from the Al contact into the ZnO conduction band, while the holes are injected into the PEDOT:PSS layer through a (~ 1.0 eV) band offset and are then transported to the light emitting layer, i.e., the PFO layer (band offset ~ 0.6 eV). The total injection barrier for the holes is therefore around 1.6 eV, and a large step is

then made by the holes to reach the PFO/ZnO interface (band offset ~ 1.8 eV), resulting in a total injection barrier of 3.4 eV for the carriers in this structure.¹⁶ This value is in good agreement with the turn-on voltage mentioned above. The I-V characteristics of the LEDs fabricated with various PFO concentrations are shown in Fig. 3(b). These characteristics show that as the PFO concentration increases from 2 mg/ml to 20 mg/ml, the turn-on voltage increases significantly and the corresponding I-V curve exhibits a relatively lower current density. This was to be expected because an increase in the PFO thickness means that the diode parasitic resistance will also increase. The increase in diode parasitic resistance can be caused by imperfections at the PFO/ZnO NR interface and/or excessive contact resistance (series resistance). As discussed earlier, at higher PFO concentrations, the fabricated thin film contains areas with hill and valley shapes, which in turn produce areas of low and high ZnO NR density, respectively. Thus, the I-V characteristics of the hybrid LEDs are affected by these density variations.

The room temperature EL spectra of the LEDs fabricated with different PFO concentrations are shown in Figs. 4(a) and 4(b). All of the EL spectra exhibited broad visible emission extending from 430 nm up to 750 nm, i.e., covering the entire visible spectrum. The EL spectra for low PFO concentrations (2-8 mg/ml) featured prominent blue peaks at 452 nm and 473 nm. The former is caused by the excitonic emission of the PFO, while the latter peak belongs to its vibronic replica.²¹ Two additional peaks were observed in the EL spectra of Figs. 4(a) and 4(b) at 508 nm and 540 nm. The emission at 508 nm can be ascribed to the electrochemical degradation of PFO during device operation. The electrons injected from the ZnO NR sides induce chemical reactions in the PFO, which causes cross-linking of the PFO chain and leads to cleavage of the σ band.

The green band emission at 540 nm is attributed to two possible sources: the first potential source is the ZnO NR deep level defect (DLE) emission which is observed

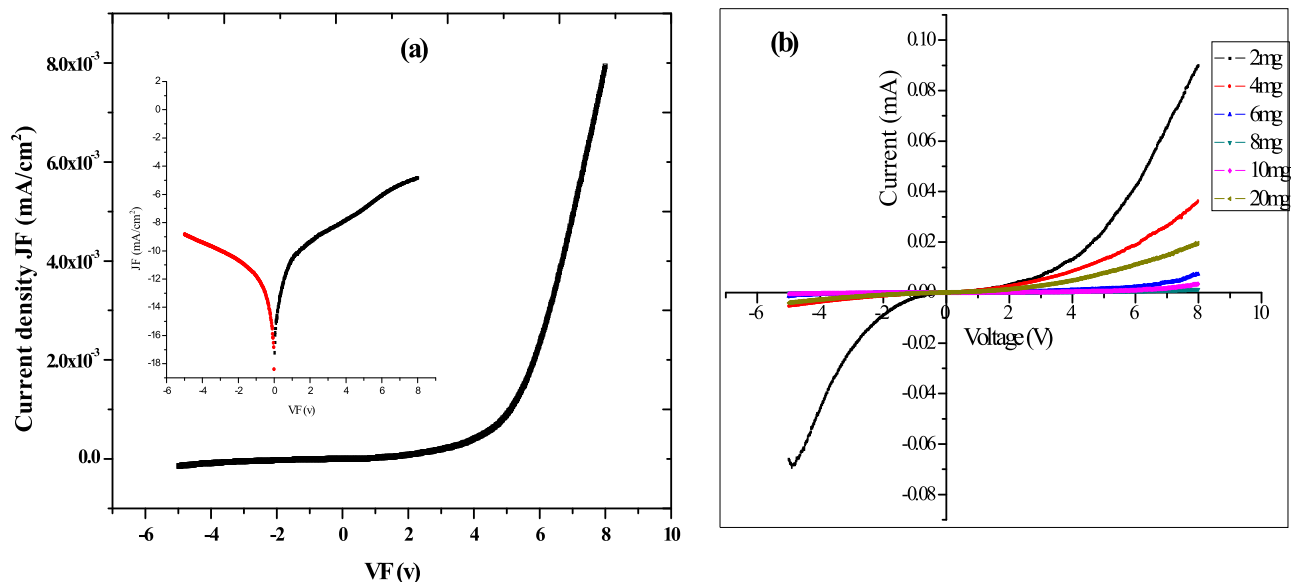


FIG. 3. (a) Current-voltage (I-V) characteristics of the fabricated LED for 2 mg/ml PFO; the inset shows the semi-log plot of the I-V characteristics. (b) I-V characteristics of ZnO NR/PFO hybrid LEDs for various PFO concentrations.

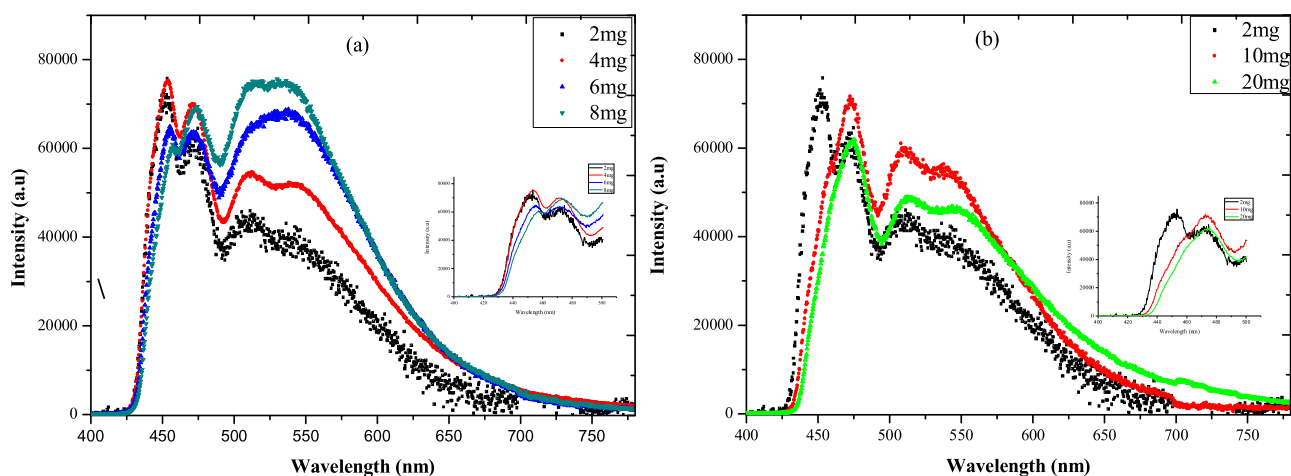


FIG. 4. (a) and (b) Electroluminescence spectra of the hybrid LEDs with PFO concentrations from 2 mg/ml to 20 mg/ml.

particularly in the low temperature grown nanorods.²² However, the origin of the DLE green band is not yet conclusively proven, because many point defects have been assigned as a potential source of the DLE emission in ZnO.² Oxygen vacancies (V_O) are one possible source of this green band emission, and zinc vacancies (V_{Zn}) with different optical characteristics have also been proposed as the origin of this broad green luminescence band in ZnO.²³ Similarly, the PFO thin film side may comprise large numbers of radiative defects. The interaction between the ZnO NR surfaces and the PFO thin films makes the PFO link up with the ZnO, which in turn leads to ZnO NR/PFO interfaces containing strong defect emissions.²⁴ The PFO defect emission is attributed to the formation of on-chain defects in the presence of oxygen or fluorenone.²⁵ The fluorenone defects are generated through the incorporation of oxygen as $O=C$ bonds in the polymer backbone, which can easily be formed by electro- (or photo-) oxidation of the polymer.²⁶ During the device fabrication processes, the PFO thin films were annealed in air to evaporate the solvents. Subsequently, the substrate coated with the PFO thin film was placed in an aqueous solution for the growth of ZnO NRs. These two device processing steps are performed in oxygen-rich environments which favor the formation of fluorenone defects. It was found that increasing the PFO concentration in the hybrid LEDs caused the EL emission spectra to change markedly, as shown in Figs. 4(a) and 4(b). The changes in the EL spectra of the PFO/ZnO LEDs can be described as follows. The dominant blue peak at 452 nm was gradually suppressed with increasing PFO concentration up to 6 mg/ml. The dominance of the peak at 473 nm started at a concentration of 8 mg/ml and continued for concentrations up to 20 mg/ml. The intensity of the broad green emission of the PFO/ZnO LEDs was also enhanced by increasing the PFO concentration. The intensity drop of the 452 nm peak can be correlated with the emergence of the β -phase (see Fig. 2) at the expense of the α -phase, as discussed earlier. The β -phase emission is very close in energy to that of the vibronic replica of the α -phase (473 nm), and as a result the glassy phase is hindered by the formation of the β -phase.²⁷ As shown in Fig. 4(a), the 452 nm peak gradually decreased for PFO concentrations up

to 6 mg/ml, and the emission from the β -phase emerges instantaneously. Figure 5(a) depicts the increases in relative intensity of the β -phase and the relative decreases of the 452 nm peak of PFO in the EL spectra; the inset shows that both the β -phase and the peak at 473 nm increased with the PFO concentration. The drop in the first peak (452 nm) of the EL spectra implies either fast and effective energy transfer from the α -phase to the β -phase domain²⁸ or that the β -phase may act as a low-energy trap for the excitons because it has a smaller energy gap when compared to the α -phase.²⁹ Both of these mechanisms result in the drop in the 452 nm peak intensity when the contribution from the β -phase in the PFO film increases. Another change which was observed in the EL spectrum is the enhancement of the green peak with increasing PFO concentration. This enhancement of the green band emission may originate from the increased quantity of fluorenone defects that were introduced by larger concentrations of PFO (in the film thickness), or from the increased density of ZnO NRs for higher PFO concentrations, or from a combination of the two effects. Two processes are involved simultaneously in the green band emission of the PFO: first, energy transfer from the excitons on the PFO main chain to the fluorenone defect sites, and second, trapping of excitons at the fluorenone defect sites followed by radiative recombination.³⁰ The fluorenone defects act as a low-energy trap, and we expect that there will be competition between the β -phase and the fluorenone defects for the excitons that were created within the PFO thin film.²⁷

The observed concentration dependent EL of the LEDs can also be explained by assuming that a ternary system exists, comprising a PFO α -phase, a β -phase and the fluorenone defects. In this case, the energy transfer can populate the double trap system to generate the EL emission spectra of the PFO/ZnO NR LEDs. Excitons are created in the α -phase and then radiatively recombine according to the (0-0) transition which produces the 452 nm peak for low PFO concentrations. At higher concentrations, these excitons are energy transferred from the α -phase to the β -phase and then recombine to produce the overlapping peak at 473 nm. The third possible path for the excitons is to be trapped in the fluorenone defect sites and then, together with the DLE ZnO

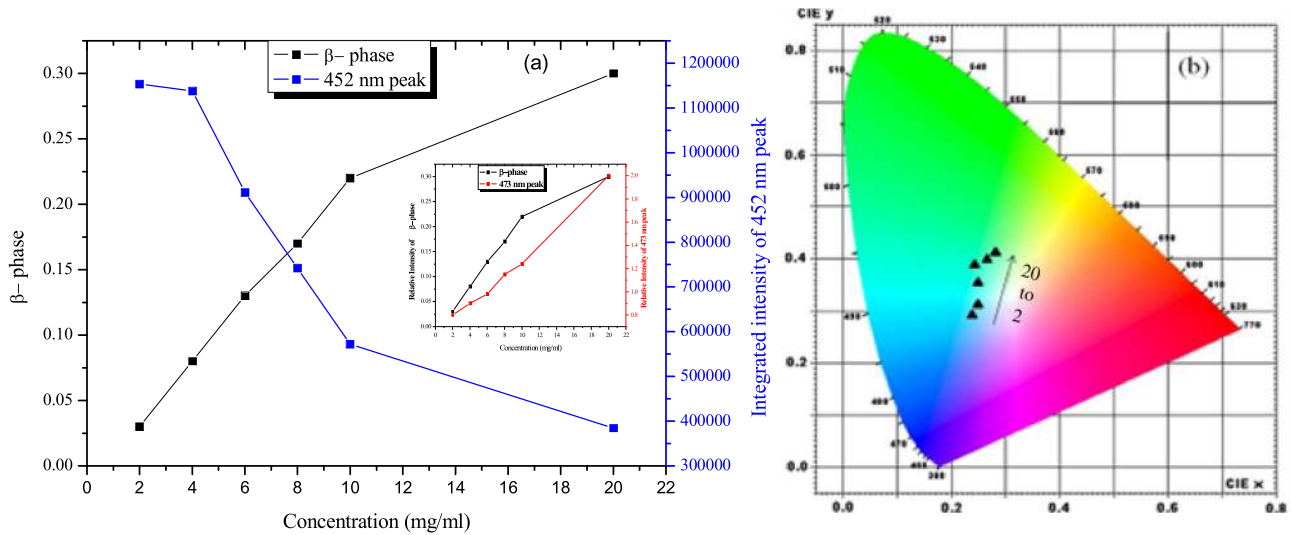


FIG. 5. (a) Integrated intensity of the blue emission peak for all LEDs, showing the reduction of the blue peak (452 nm) and the increased relative intensity of the β -phase at higher PFO concentrations; the inset shows the peak at 473 nm increasing with increasing β -phase. (b) Chromaticity diagram (CIE coordinates) for all fabricated LEDs showing the emission color change from bluish to greenish white.

NRs, enhance the green emission of the hybrid LEDs. This last process is responsible for the quenching of the blue emission.

The corresponding Commission Internationale de l’Eclairage (CIE) chromaticity coordinates of the spectra at different concentrations are shown in Fig. 5(b). The emission color of the LEDs changes from bluish-white with color coordinates (0.259, 0.312) to a greenish-white (0.309, 0.418) with increasing PFO concentration, while the correlated color temperature (CCT) decreases from 11741 K to 6196 K.

To explore our previous assignment on the effects of the injected carriers on defect emissions of PFO caused by electrochemical oxidation of the polymer chains, we performed current dependent EL measurements. The EL spectra of the LEDs with the lowest (2 mg/ml) PFO concentration were measured at injected currents of 0.3 mA, 0.6 mA, 2.3 mA, and 5.0 mA for a fixed applied voltage of 15 V. The results are shown in Fig. 6(a) for only the lowest and highest

injected currents, while the corresponding CIE diagram for these LEDs is depicted in Fig. 6(b). Interestingly, at low injection currents (0.3-0.6 mA), the EL spectrum shows the blue peaks that are identical to those discussed earlier, i.e., at 452 nm and 470 nm. The EL also exhibited a broad green band related to the radiative defects in the PFO/ZnO hybrid LED as discussed above. When the injected current was increased further to 2.3-5 mA, a new peak at 465 nm emerged in the EL spectra (Fig. 6(a)). Figure 6(a) also shows that the green band emission at 540 nm becomes higher than that of the blue peak. At low injection currents, electron-hole recombination occurs at the PFO/ZnO NR interfaces. When the injection current increases, the electron density also increases and more carriers accumulate at the PFO/ZnO interface. The accumulated electrons promote the degradation of the LEDs by electrochemical oxidation of the PFO thin film.³¹ The appearance of the 465 nm peak in the EL of the PFO based devices thus arises from new chemical

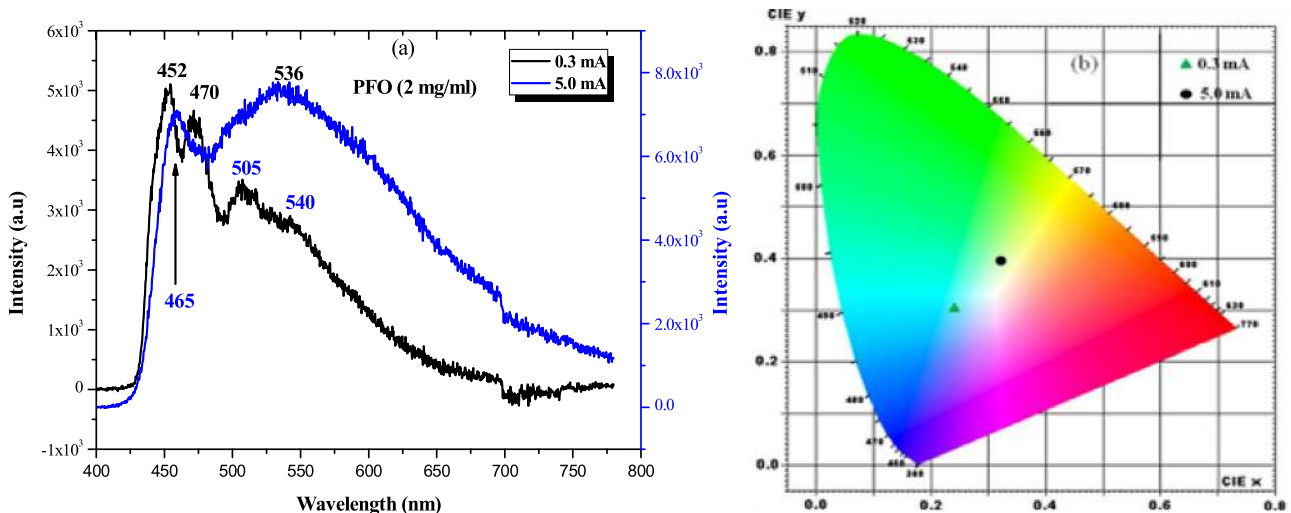


FIG. 6. (a) Electroluminescence spectra of the ZnO NR/PFO (2 mg/ml) LED at low and high injection currents. (b) Chromaticity diagram of the corresponding LED.

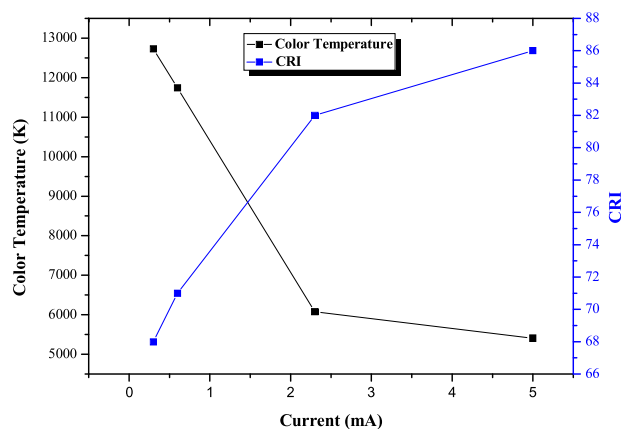


FIG. 7. The effect of different injection currents on the CRI and the CCT.

species that appear as a result of an excess of electrons.²⁶ This is ascribed to the fact that the electron mobility in ZnO NRs is higher than the hole mobility in PFO.²⁴ Electrons at high injection currents directly traverse at the PFO/ZnO interface and because the PFO layer is sufficiently thin (29.1 nm), the probability of an electron recombining with a hole at the PFO side becomes a minimum. This will favor an accumulation of electrons at the PFO/PEDOT:PSS interface, which may shift the recombination zone towards this interface. The green emission peak at 540 nm is also enhanced and becomes higher than the blue emission peak under high injection currents. The current flow through the polymer is also believed to play a crucial role in the oxidation of the polymer.³² During the electro-oxidation process of PFO, fluorenone defects are formed which in turn increase the green emission over the blue emission.³³

Changing the injected current affects the color rendering index (CRI) and the CCT, as shown in Fig. 7; at low currents (<1 mA), the CCT is a maximum and the CRI is a minimum, and increasing the injection current causes the CCT to decrease and the CRI to increase. By increasing the injection current, the green emission peak is enhanced and broadens because of the oxidation of the PFO and/or the DLE of the ZnO NRs, which results in an improved CRI, which increased from 68 to 86 with increasing injection current from 0.3 mA to 5.0 mA. This indicates that the LEDs operating at higher injection currents come closer to natural white light. Conversely, the CCT falls from 12731 K to 5042 K, which shows that the fabricated hybrid LEDs give an impression of cold light at low injection currents and an impression of warm light at high injection currents.

IV. CONCLUSION

We have demonstrated white light emission from PFO/ZnO NR hybrid LEDs grown on a plastic substrate at 50 °C. Analysis of the EL spectra reveals that the emission spectra of hybrid LEDs can be tuned from a bluish white to a greenish white by increasing the PFO concentration. The trapping of excitons in the β -phase and by the fluorenone defects results in the reduction of the blue peak at 452 nm and the enhancement of the green emission band at higher PFO concentrations. The chromaticity coordinates, the CRI and the

CCT also varied for devices with different PFO concentrations. Also, the EL spectra under different injection currents show that because of electro-oxidation of the PFO at higher currents, a new peak appears at 465 nm together with an enhancement of the green emission band. Our results show that tunable emission spectra can be obtained by varying the polymer concentration and increasing the injection current.

- ¹C. Klingshirn, *Phys. Status Solidi B* **244**(9), 3027 (2007).
- ²Ü. Özgür, Ya. I. Alivov, C. Liu, A. Teke, M. A. Reshchikov, S. Doğan, V. Avrutin, S. J. Cho, and H. Morkoç, *J. Appl. Phys.* **98**(4), 041301 (2005).
- ³L. Vayssieres, *Adv. Mater.* **15**(5), 464 (2003).
- ⁴A. Zainelabdin, S. Zaman, G. Amin, O. Nur, and M. Willander, *Cryst. Growth Des.* **10**(7), 3250 (2010).
- ⁵R. Könenkamp, R. C. Word, and C. Schlegel, *Appl. Phys. Lett.* **85**(24), 6004 (2004).
- ⁶C. S. Rout and C. N. Rao, *Nanotechnology* **19**(28), 285203 (2008).
- ⁷L. Qian, Y. Zheng, K. R. Choudhury, D. Bera, F. So, J. Xue, and P. H. Holloway, *Nano Today* **5**(5), 384 (2010).
- ⁸R. Kumar, N. Khare, V. Kumar, G. L. Bhalla, R. Srivastava, G. Chauhan, and M. N. Kamalasanan, *Semicond. Sci. Technol.* **24**(4), 045020 (2009).
- ⁹T. Zhang, Z. Xu, L. Qian, D. L. Tao, F. Teng, and X. R. Xu, *Opt. Mater.* **29**(2–3), 216 (2006).
- ¹⁰S.-R. Tseng, S.-Y. Li, H.-F. Meng, Y.-H. Yu, C.-M. Yang, H.-H. Liao, S.-F. Horng, and C.-S. Hsu, *J. Appl. Phys.* **101**(8), 084510 (2007).
- ¹¹H. T. Nicolai, G. A. H. Wetzelaer, M. Kuik, A. J. Kronemeijer, B. de Boer, and P. W. M. Blom, *Appl. Phys. Lett.* **96**(17), 172107 (2010).
- ¹²P. Chen, G. Yang, T. Liu, T. Li, M. Wang, and W. Huang, *Polym. Int.* **55**(5), 473 (2006).
- ¹³M. T. Bernius, M. Inbasekaran, J. O'Brien, and W. Wu, *Adv. Mater.* **12**(23), 1737 (2000).
- ¹⁴D. Look, *J. Electron. Mater.* **35**(6), 1299 (2006).
- ¹⁵N. Bano, S. Zaman, A. Zainelabdin, S. Hussain, I. Hussain, O. Nur, and M. Willander, *J. Appl. Phys.* **108**(4), 043103 (2010).
- ¹⁶S. Zaman, A. Zainelabdin, G. Amin, O. Nur, and M. Willander, *Appl. Phys. A* **104**(4), 1203 (2011).
- ¹⁷D. Rickard, S. Giordani, W. J. Blau, and J. N. Coleman, *J. Lumin.* **128**(1), 31 (2008).
- ¹⁸M. Misaki, M. Chikamatsu, Y. Yoshida, R. Azumi, N. Tanigaki, K. Yase, S. Nagamatsu, and Y. Ueda, *Appl. Phys. Lett.* **93**(2), 023304 (2008).
- ¹⁹S. Gamerith, C. Gadermaier, U. Scherf, and E. J. W. List, *Phys. Status Solidi A* **201**(6), 1132 (2004).
- ²⁰B. K. Sharma, N. Khare, and S. Ahmad, *Solid State Commun.* **149**(19–20), 771 (2009).
- ²¹A. Wadeasa, O. Nur, and M. Willander, *Nanotechnology* **20**(6), 065710 (2009).
- ²²A. B. Djurišić and Y. H. Leung, *Small* **2**(8–9), 944 (2006).
- ²³M. Willander, O. Nur, J. R. Sadaf, M. I. Qadir, S. Zaman, A. Zainelabdin, N. Bano, and I. Hussain, *Materials* **3**(4), 2643 (2010).
- ²⁴C. Y. Lee, J. Y. Wang, Y. Chou, C. L. Cheng, C. H. Chao, S. C. Shiu, S. C. Hung, J. J. Chao, M. Y. Liu, W. F. Su, Y. F. Chen, and C. F. Lin, *Nanotechnology* **20**(42), 425202 (2009).
- ²⁵X. Gong, P. K. Iyer, D. Moses, G. C. Bazan, A. J. Heeger, and S. S. Xiao, *Adv. Funct. Mater.* **13**(4), 325 (2003).
- ²⁶F. Montilla and R. Mallavia, *Adv. Funct. Mater.* **17**(1), 71 (2007).
- ²⁷B. Arredondo, B. Romero, A. Gutiérrez-Llorente, A. I. Martínez, A. L. Álvarez, X. Quintana, and J. M. Otón, *Solid-State Electron.* **61**(1), 46 (2011).
- ²⁸M. Ariu, M. Sims, M. D. Rahn, J. Hill, A. M. Fox, D. G. Lidzey, M. Oda, J. Cabanillas-Gonzalez, and D. D. C. Bradley, *Phys. Rev. B* **67**(19), 195333 (2003).
- ²⁹C. Rothe, S. King, F. Dias, and A. Monkman, *Phys. Rev. B* **70**(19), 195213 (2004).
- ³⁰M. Kuik, G.-J. A. H. Wetzelaer, J. G. Laddé, H. T. Nicolai, J. Wildeman, J. Sweelssen, and P. W. M. Blom, *Adv. Funct. Mater.* **21**(23), 4502 (2011).
- ³¹B. Romero, B. Arredondo, A. L. Alvarez, R. Mallavia, A. Salinas, X. Quintana, and J. M. Otón, *Solid-State Electron.* **53**(2), 211 (2009).
- ³²I. Ugarte, W. Cambarau, C. Waldauf, F. L. Arbeloa, and R. Pacios, *Org. Electron.* **10**(8), 1606 (2009).
- ³³Y. H. Kim and D. A. Vanden Bout, *Appl. Phys. A* **95**(1), 241 (2008).